Photoionization of Highly Charged Ions Using an ECR Ion Source and Undulator Radiation

J.-M. Bizau, J.-M. Esteva, D. Cubaynes, and F. J. Wuilleumier
Laboratoire de Spectroscopie Atomique et Ionique, Université Paris-Sud, UMR CNRS No. 8624, Campus d'Orsay, B. 350, 91405 Orsay, France

C. Blancard, A. Compant La Fontaine, C. Couillaud, and J. Lachkar
Commissariat à l'Energie Atomique, DIF/DPTA, BP 12, 91680 Bruyères-le-Châtel, France

R. Marmoret, C. Rémond, and J. Bruneau
Commissariat à l'Energie Atomique, DIF/DCRE, BP 12, 91680 Bruyères-le-Châtel, France

D. Hitz, P. Ludwig, and M. Delaunay
Département de Recherche Fondamentale sur la Matière Condensée-SI2A, CEA-Grenoble, 17 rue des Martyrs, 38054 Grenoble Cedex 9, France
(Received 12 July 1999)

Photoionization of Xe^{4+} to Xe^{7+} ions was studied by combining an electron cyclotron resonance ion source with synchrotron radiation. Multiconfiguration Dirac-Fock calculations were performed to interpret the data. Many autoionization lines were measured and identified, resulting from excitation of a $4d$ electron into nf and np orbitals followed by Auger decay of the excited states. Continuum photoionization is negligible for the higher members of the isonuclear series.

PACS numbers: 32.80.Fb, 32.80.Hd

In this Letter, we present the results of new experiments investigating the photoionization of highly charged ions produced by an electron cyclotron resonance (ECR) ion source. Single and double ionization of Xe^{4+} ions was studied using photon beams of undulator synchrotron radiation (SR) between 60 and 160 eV photon energy, revealing the existence of a large number of resonant transitions in which a $4d$ electron is excited into np and nf orbitals. Single photoionization of Xe^{5+}, Xe^{6+}, and Xe^{7+} ions was also measured, allowing us to observe intense $4d \rightarrow nf$ transitions. To interpret the data, a multiconfiguration Dirac-Fock code was used to calculate the energies and the oscillator strengths of the $4d$-excitation transitions, and helped to identify most of the resonances experimentally observed in the spectra. Our results provide a complete picture of the effect of the change in the electronic charge along an isonuclear series of a multiply charged ion.

Photoionization experiments on multiply charged ions are of importance for atomic theory to test correlation and relativistic effects along isonuclear and isoelectronic series, and to provide useful data for plasmas physics and astrophysics. Experimental studies have been hampered, however, by the difficulty in producing high enough density beams of multiply charged ions. Most of the information has been obtained so far from time-resolved absorption experiments using two synchronized laser pulses [1,2]. The method has been widely used to investigate photoionization of relatively low-Z ions in low charge states, and to follow the collapse of some specific wave functions along isoelectronic and isonuclear sequences involving $4d$ excitation in neighboring elements [3–5].

The first measurements of photoionization cross sections on singly charged ions using SR were achieved by photoion spectrometry [6]. Then, photoelectron spectroscopy provided results on Ca^{+} and Xe^{+} ions [7–9]. Renewed efforts to exploit storage rings for the investigation of photoionization in ions have recently succeeded in providing detailed results for a few singly charged ions [10,11] and for the doubly charged Xe^{2+} ion [12], and in obtaining preliminary results for the Xe^{3+} ion [13]. This Letter reports a significant new step in highly charged ion physics by investigating the complete stripping of an atomic shell electron by electron.

Because of the lack of experimental data, the main source of information on multiply charged ions was, for a long time, tables [14,15] reporting the results of theoretical one-electron calculations for photoabsorption and photoionization cross sections up to $Z = 30$. Later, the use of correlated wave functions allowed some tests of the validity of the one-electron model [16]. An international effort was also developed in the Opacity Project [17], whose aim is to calculate accurately the opacities in stellar envelopes.

In the work presented here, we chose to address a physical problem requiring experimental investigation over a wide range of charge states in multiply charged ions. We concentrated on photoionization processes involving $4d$ electrons along the isonuclear series of xenon. For neutral xenon (Xe I) atoms, there have been many photoionization studies on the $4d \rightarrow \varepsilon f$ cross section since the first photoabsorption measurement [18]. The existence of a broad resonance in the $4d$ cross section was explained within the one-electron model [19], although

0031-9007/00/84(3)/435(4)$15.00

the absolute values of the cross section and the energy position of the maximum could be reproduced theoretically only when correlation and polarization effects were fully accounted for [20]. The qualitative explanation resides in the existence of a double well for the effective potential [21,22]. In Xe I, the main part of the $4f$-wave function resides in the outer well. Therefore, the overlap of the bounded $4d$ orbital is much larger with the εf continuum wave function than with the empty $4f$ orbital, explaining the weak intensity of the discrete $4d \rightarrow nf$ transitions. An efficient way to induce changes in the effective atomic potential is to remove one or several electrons from the outer shell. Recent measurements [12,13] have suggested that the $4f$ orbital is already mostly localized in the inner well for Xe^{2+}. Preliminary results on Xe^{3+} ions [13] indicate that the discrete structures near the $4d$ threshold dominate over direct photoionization of $4d$ electrons, as was already observed in Ba^{2+} ions [4].

In our investigation, we studied photoionization of ions over the isonuclear series of xenon, from Xe^{+} to Xe^{7+}, thus providing a complete picture of the charge-state dependence of the observed features. Our data for Xe^{+} to Xe^{3+} ions confirm the previous observations [11–13]. Here, we present results for the higher members of the series, i.e., for Xe^{4+} to Xe^{7+} ions. The experiments were performed at the SR source Super-ACO. The main novelty in our experimental setup is the ECR ion source used to provide beams of highly charged ions for SR studies, as was already suggested some years ago [23]. The ECR source used is a compact 10 GHz permanent magnet source providing, in the interaction region, electrical currents of about 100 nA for ionic charges up to 8+. After extraction and charge selection by a Wien filter, the ions are decelerated before being deflected by a quadrupolar electrostatic deflector. Their trajectory is then colinear, over an interaction length of 20 cm, with the monochromatized photon beam emitted by the SU6 undulator. After deflection by a variable electrostatic field, the ions are counted with a multichannel plate array. A chopper allows us to record the ion signal measured with and without photons and to determine the contribution of collisional processes to the measured data. In our experiments, we tuned the energy of the photon beam over the 60–160 eV energy range with a spectral resolution varying between 0.15 and 1.0 eV.

To interpret the data, we used a multiconfiguration Dirac-Fock (MCDF) code [24], accounting for the Breit interaction and for radiative and finite nuclear mass corrections. This program has been used to calculate energy levels, and photoexcitation and photoionization cross sections. Calculations of the decay rates were also performed, showing that the Auger rates are larger than the radiative rates by a factor of 100 to 1000. For the calculations of the $4d$-excitation spectrum, we described the initial states by the following configurations: $[4d^{10}]$-$5s^2 5p^2$ for Xe^{4+}, -$5s^2 5p$ for Xe^{5+}, -$5s^2$ for Xe^{6+}, and -$5s$ for Xe^{7+}. In the operating mode of our ECR source [25], we assumed statistical populations of the initial levels for a given ionic stage. For Xe^{4+}, we checked that introducing an additional configuration ($5s^2 5p^2$ and $5p^2 5d^2$) has a negligible effect on the results. We constructed the excited states from the $4d^9 5s^m 5p^{m'} np$ ($n = 5$–7) and $4d^9 5s^m 5p^{m'} nf$ ($n = 4$–7) configurations, with $m = 1$ and 2, and $m' = 2, 1$, and 0. The oscillator strengths were calculated using the velocity form of the electric dipolar operator. To compare the results of our calculations with experiment, we assumed a Lorentzian profile for the shape of each excitation line due to the finite lifetime of the state [we fixed a full width at half maximum (FWHM) of 100 meV, close to the value of the $4d$ width in neutral xenon]. Then, the resulting theoretical spectra was convolved with a Gaussian profile accounting for the instrumental function (0.2–0.5 eV FWHM).

As an example of our results, we show in Fig. 1 (upper panel) the variation of the cross sections for single and double ionization of Xe^{4+} ions. Because of the lack of information on the overlap of the photon and ion beams, our experimental results are given in arbitrary units.

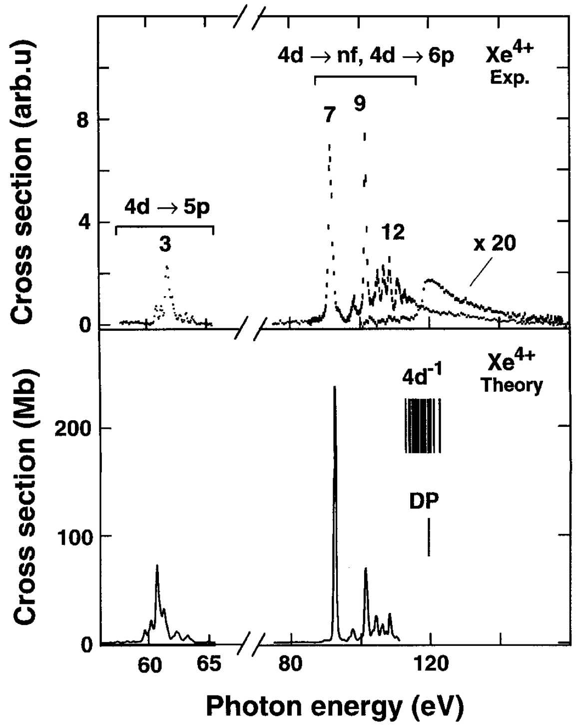

FIG. 1. Experimental spectra for single and double ionization of Xe^{4+} ions. The discrete lines result from autoionization of Xe^{4+} excited states, the continuous lines from single $4d$ photoionization of part of the Xe^{4+} ions (see text), and from the Auger decay (×20) of the core-ionized Xe^{5+} ions. The results of our MCDF calculations for the $4d$ excitations in Xe^{4+} are shown in the lower panel. DP identifies the double ionization threshold.

The single photoionization spectrum (resulting from measurements of the Xe^{5+} signal) shows many discrete lines followed by a continuum on the high-photon-energy side. The weak double ionization spectrum (measured from the Xe^{6+} signal) is displayed with a magnification factor of 20. Its intensity rises from the double ionization threshold and then decreases continuously with increasing photon energy. The lines with significant intensity are numbered in sequence. In the lower panel of Fig. 1, we show the results of our theoretical calculations. The spectrum results from the addition of the calculated intensities of all possible transitions from the $4d^{10}5s^25p^2\,{}^3P_0$, ${}^3P_1$, ${}^3P_2$, ${}^1D_2$, and ${}^1S_0$ initial levels. The calculated position of the many $4d$-ionization thresholds is indicated by vertical bars. Note that most of the energies of the $4d$-ionization thresholds are lower than the double ionization (DP) threshold.

Below the $4d$-ionization thresholds, the final states of Xe^{5+} can be reached by following two different ways. The first way follows the resonant excitation of a $4d$ electron into np ($n \geq 5$) or nf ($n \geq 4$) orbitals, populating intermediate Xe^{4+*} excited states followed by autoionization in final states of Xe^{5+}. The second way is the $5p$ or $5s$ photoionization of the Xe^{4+} ions. Our measurements show that the resonant way is the dominant one. The route followed to reach the $4d^{10}5s^2\,{}^1S_0$ Xe^{6+} final state proceeds via single photoionization of a $4d$ electron, leaving the intermediate Xe^{5+} states in a $4d^95s^25p^2$ configuration. The core-ionized Xe^{5+} states whose excitation energies are higher than the energy of the DP threshold can then decay by Auger relaxation into the ground state of Xe^{6+}. The other $4d$ core-ionized Xe^{5+} states can decay only by radiative transitions. Our measurements indicate that the dominant processes are the discrete excitations of a $4d$ electron into np and nf empty orbitals, and they confirm that most of the oscillator strength is now concentrated in the discrete part of the spectrum.

Our experimental and theoretical results are in good agreement for the general shape of the spectrum, although the relative intensities differ for some of the discrete lines. The theoretical energy values of the most intense resonant structures differ usually by no more than 1 eV from the experimental results, and some times by much less. It should be noted that each observed resonance line is not due to a single excitation transition but to the sum of several transitions which are not experimentally resolved. The most intense line (7) results from the decay of many excited states built on a strong mixing of the $[4d^95s^25p^2]$-$4f$ -$6p$, and -$5f$ configurations. The $4d \rightarrow nf$ transitions have the highest oscillator strengths and form Rydberg series (e.g., $4d \rightarrow 5f$ and $6f$, lines 9 and 10, respectively), converging to the $4d$-ionization thresholds of Xe^{4+}. One can note, however, the large difference between the measured and calculated intensities of the second member of the series (line 9). Preliminary calculations seem to indicate that this difference could be accounted for by strong differences in the autoionization rates of the $[4d^95s^25p^2]$-$4f$ and -$5f$ states. We also calculated transitions from metastable states with a $4d^{10}5s^25p4f$ configuration and can conclude that their contribution is weak in the experimental spectrum.

In Fig. 2, we show the single photoionization spectra for the higher members of the isonuclear sequences, i.e., Xe^{5+}, Xe^{6+}, and Xe^{7+}, and in Fig. 3 our theoretical results. The $4d \rightarrow nf$ series dominates the spectra. The intensities of these resonance lines decrease regularly with increasing values of the principal quantum number of the excited electron. For Xe^{6+}, we checked that the signal due to single photoionization is negligible above the $4d$ ionization thresholds within our detection sensitivity. For Xe^{5+}, we did not measure any signal in the double photoionization continua, which confirms that direct double photoionization in the outer shell is negligible. The theoretical results are in very good agreement with the experiment for Xe^{5+} and Xe^{6+} ions, but, in Xe^{7+}, the line due to $4d \rightarrow 4f$ excitation is missing in the experimental spectrum. The explanation

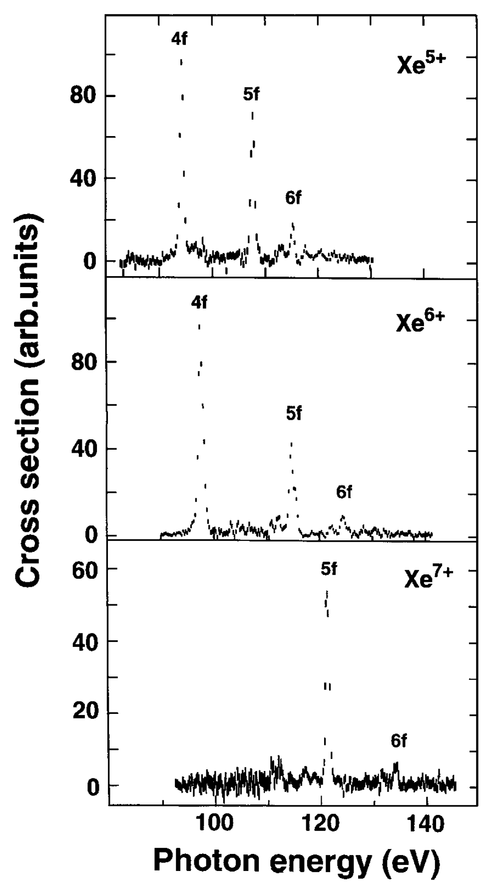

FIG. 2. Experimental single photoionization spectra of Xe^{5+}, Xe^{6+}, and Xe^{7+} measured below the $4d$-ionization thresholds. Autoionization lines following $4d \rightarrow nf$ excitations dominate the spectrum. Weaker lines are due to the decay of excited states formed by $4d \rightarrow np$ ($n > 5$) excitations.

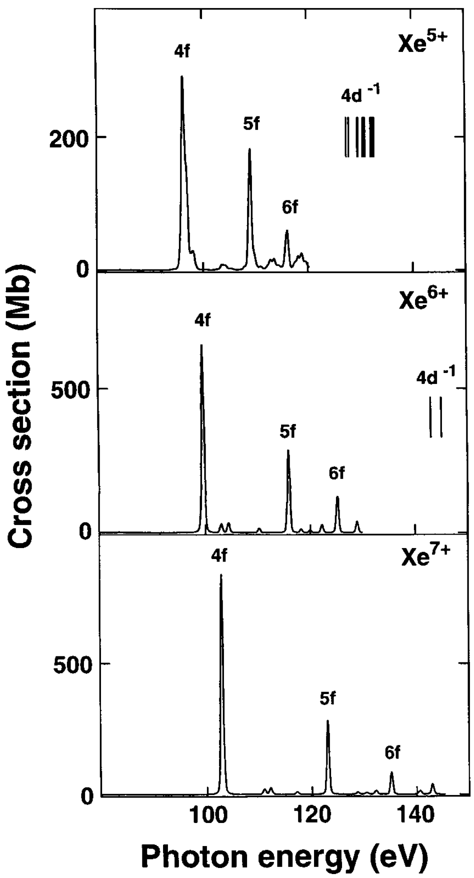

FIG. 3. Photoexcitation spectra of Xe^{5+}, Xe^{6+}, and Xe^{7+} resulting from our MCDF calculations.

for this apparent disagreement is simply that the energies of the Xe^{7+} $4d^9 4f 5s$ excited states are lower, by more than 1 eV, according to our calculations, than the energy of the Xe^{8+} $4d^{10}\,{}^1S_0$ state, and then these excited states cannot autoionize. Thus, the overall agreement between theory and experiment is excellent.

In conclusion, we have succeeded in measuring photoionization spectra of highly charged ions using ion beams from an ECR ion source and photon beams delivered by an undulator. The MCDF calculations for the Xe^{4+} to Xe^{7+} sequence are in good agreement with the experimental observations. Our results provide a complete picture of the behavior of resonant and continuum photoionization processes along an isonuclear sequence.

We thank M. Druetta for assistance in using the ECR source and T. Morgan and E. Kennedy for critical reading of the manuscript.

[1] T. B. Lucatorto and T. J. Mc Ilrath, Phys. Rev. Lett. **37**, 428 (1977).
[2] J. T. Costello *et al.*, Phys. Scr. **T34**, 1068 (1991), and references therein.
[3] G. O'Sullivan *et al.*, Phys. Rev. A **53**, 3211 (1996).
[4] T. B. Lucatorto *et al.*, Phys. Rev. Lett. **47**, 1124 (1981).
[5] U. Köble *et al.*, Phys. Rev. Lett. **74**, 2188 (1995).
[6] I. Lyon *et al.*, J. Phys. B **20**, 1471 (1987), and references therein.
[7] J.-M. Bizau *et al.*, Phys. Rev. Lett. **67**, 576 (1991).
[8] S. Al Moussalami *et al.*, Phys. Rev. Lett. **76**, 4496 (1996).
[9] A. Gottwald, C. Gerth, and M. Richter, Phys. Rev. Lett. **82**, 2068 (1999).
[10] T. Koizumi *et al.*, J. Phys. B **28**, 609 (1995).
[11] M. Sano *et al.*, J. Phys. B **28**, 5305 (1996).
[12] N. Watanabe *et al.*, J. Phys. B **31**, 4137 (1998).
[13] T. Koizumi *et al.*, Phys. Scr. **T73**, 131 (1997).
[14] R. F. Reilmann and S. T. Manson, Astrophys. J. Suppl. Ser. **40**, 815 (1979).
[15] D. A. Verner *et al.*, At. Data Nucl. Data Tables **55**, 233 (1993).
[16] G. Nasreen, R. Desmukh, and S. T. Manson, J. Phys. B **21**, L281 (1988).
[17] J. M. Seaton, J. Phys. B **20**, 6363 (1987).
[18] D. L. Ederer, Phys. Rev. Lett. **13**, 760 (1964).
[19] J. W. Cooper, Phys. Rev. Lett. **13**, 762 (1964).
[20] M. Ya Amusia *et al.*, J. Phys. B **23**, 393 (1990).
[21] J. P. Connerade, Contemp. Phys. **19**, 415 (1978), and references therein.
[22] K. T. Cheng and W. R. Johnson, Phys. Rev. A **28**, 2820 (1983).
[23] F. J. Wuilleumier, in *Laser Techniques in the Extreme Ultraviolet*, edited by S. E. Harris and T. B. Lucatorto, AIP Conf. Proc. No. 119 (AIP, New York, 1984) p. 220.
[24] J. Bruneau, J. Phys. B **16**, 4135 (1983).
[25] D. Hitz, R. Berreby, and M. Druetta, Phys. Scr. **T80**, 511 (1999).